Environmental Modelling and Software 186 (2025) 106354

Contents lists available at ScienceDirect

Environmental Modelling and Software

journal homepage: www.elsevier.com/locate/envsoft

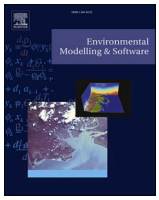

A simple method for the enhancement of river bathymetry in LiDAR DEM

Gabriele Farina [a], Marco Pilotti [a,*], Luca Milanesi [b], Giulia Valerio [a]

[a] Università degli Studi di Brescia, Italy
[b] Consorzio Irrigazioni Cremonesi, Italy

ARTICLE INFO

Keywords:
Shallow Water Equations
Bathymetry Correction
LiDAR
Digital Elevation Model

ABSTRACT

The preparation of an accurate bathymetry is crucial for flood modeling and is usually done using a LiDAR-derived Digital Elevation Model (DEM). However, a recurrent flaw of LiDAR DEM is the presence of water along rivers, that prevents a careful reproduction of the river bed and channel conveyance. This paper provides a simple and effective algorithm to tackle this problem when ground surveyed cross sections are available to complement DEM data. In contrast to most interpolation approaches, the algorithm is physically-based, using a 2D Shallow Water Equations solver in the identification of the wetted river bed perimeter. The method was applied to a 37 km long stretch of the Mella River (Northern Italy) providing satisfactory results. Further examples show the potential of the method in cases of increasing complexity of riverbed bathymetry. The procedure is explained step by step in the supplementary material, using two widely used freeware software.

1. Introduction

An accurate bathymetric description of the floodplain, the watercourse, and the transversal hydraulic structures are fundamental requirements for the careful reproduction of the propagation of floods with Shallow Water Equations (SWE) (e.g., Pilotti, 2016; Bures et al., 2019), and the preparation of a good bathymetry is often the most time-consuming effort in the whole modeling process. The approach currently used for producing high resolution DEM is Light Detection And Ranging (LiDAR) that, along watercourses, is hindered by the presence of vegetation and water (e.g., Mazzoleni et al., 2020). In order to limit the hiding effect of vegetation on the underlying terrain, aerial surveys should be accomplished in non-vegetative period and ground reflection from the first signal must be singled out using filtering algorithms. However, LiDAR sensors typically used for fluvial application operate with near-infrared radiation mostly absorbed by the water column (Kinzel et al., 2013). Accordingly, the survey should be carried out during low-flow periods along with the preferential use of green light laser, capable of penetrating shallow clear water. Finally, also steep banks of artificial canals could hide the actual bottom of the LiDAR beam. Accordingly, in spite of all the precautions, ordinary LiDAR can still misrepresent the bathymetry of watercourses, and a naïve use of LiDAR data could show up unrealistically low watercourses conveyance.

In literature, several methods are proposed to tackle the problem of river bathymetry enhancement, sometimes requiring complex post-processing with proprietary codes. Mainly, there are two possibilities, which rely on the availability of surveyed cross section (CS_{sur}, in the following) whose optimal location for river modeling purposes can be selected according to different criteria that have been proposed in the literature (e.g., Castellarin et al., 2009; Conner and Tonina, 2014). If a set of CS_{sur} is available, the standard solution to LiDAR enhancement consists in creating a DEM of the river bed by interpolating CS_{sur} and substituting it into the original DEM. In literature, different methods for the interpolation of surveyed cross sections were proposed (e.g., Caviedes-Voullième et al., 2014; Dysarz, 2018; Merwade et al., 2008; Lai et al., 2018). The interpolation of the cross sections along the river centerline can also be effectively implemented in 2D hydraulic modeling software (e.g., HEC-RAS, Brunner, 2024, that we successfully used in many cases, e.g., Pilotti et al., 2020; Milanesi and Pilotti, 2021) to assist the user in the bathymetry reconstruction, reducing the number of operations, time and potential errors. Although these algorithms in many situations can be very effective, providing a careful reproduction of the channel bed, in other situations they could lead to an inaccurate reconstruction of the intermediate bathymetry. For instance, 1) when an intermediate island is not accounted by two following cross sections, it is missed in the reconstructed bathymetry if not integrated with a specific technique (Merwade et al., 2008); conversely, 2) if a cross section intersects the profile of elevated ground emerging from water, this is

* Corresponding author.
E-mail addresses: gabriele.farina@unibs.it (G. Farina), marco.pilotti@unibs.it (M. Pilotti), direttore@consorzioirrigazioni.it (L. Milanesi), giulia.valerio@unibs.it (G. Valerio).

https://doi.org/10.1016/j.envsoft.2025.106354
Received 23 October 2024; Received in revised form 23 January 2025; Accepted 27 January 2025
Available online 1 February 2025

interpolated as far as the following CS in the recreated bathymetry, extending a local morphological feature to the whole reach between the 2 CSs; 3) the interpolation uses an average bed slope between two CSs, so neglecting the local slope variation and creating interpolated CSs that could be above or below the local thalweg. Sometimes the modification can be hydraulically relevant (e.g., when a bed drop is present between two CSs or the two CSs are separated by a long river stretch, maybe characterized by variable slope) creating CSs that do not fit the surrounding floodplain; 4) in some algorithms, the CSs interpolation can create void regions or regions superimposed to the river bed banks, creating inconsistencies between the interpolated surface and the surrounding DEM that must be suitably dealt with (Caviedes-Voullième et al., 2014; Merwade et al., 2008). In other algorithms (e.g., HEC-RAS), the user can select polylines corresponding to the banks to guide the interpolation but, however, the elevation of the CS end-points is determined by the interpolation, recreating a potential inconsistency similar to the one described in 3).

On the other hand, although LiDAR intensity returns could be used to distinguish accurately between water (weak signal) and non-water (strong signal), this information is often not available to the final user of a DEM and, accordingly, cannot practically be used to devise a procedure that identifies the water edge boundaries (e.g., Legleiter, 2012). Similarly, the use of satellite images that could theoretically be used to this purpose (Lai et al., 2021) is conditioned, among others, by space resolution issues and by the synchronicity between the survey and the satellite images.

When CS_{sur} are not available, some bathymetric correction procedures are based on estimates of the water normal depth using Manning equation, coupled with simplified transversal geometry and a reasonable discharge value (e.g., Roub et al., 2012; Bhuyian et al., 2015). Although this method can sometimes be effective (e.g., Reil et al., 2018; Bures et al., 2019), it is limited by the arbitrary hypothesis of normal flow, by knowledge of the Manning coefficient and of the river discharge at the time of the survey, that could be loosely estimated as a function of the drained area (e.g., Leopold and Maddock, 1953; Knighton, 1998) or from measured stage-discharge curves (Bhuyian et al., 2015) or remote sensing observations (e.g., Tarpanelli et al., 2021). Theoretically, the water depth could also be estimated on the basis of satellite survey (e.g., Mersel et al., 2013), but these should be synchronous to the LiDAR survey, reducing the practical applicability of this methodology to very few cases.

This paper provides an alternative method to improve the description of the river bathymetry that endeavors to exploit all the morphological information contained in the original DEM, to the point that the advantage of the proposed method grows with the morphological complexity of the river bed. Accordingly, the method is suitable for braided rivers too, where it can automatically single out sandbars as inner boundaries, a notoriously challenging task for any existing automatic tool (e.g., Lai et al., 2021).

The proposed method requires 1) a DEM properly filtered from vegetation; 2) a set of topographically-surveyed CS_{sur}, to be manipulated using a GIS software; 3) a 2D SWE solver. A reasonable guess on a suitable low-flow discharge value is also needed.

The procedure modifies the DEM on the basis of the "true" information contained in the surveyed CS_{sur}. The comparison of CS_{sur} with the corresponding ones extracted from the original DEM provides the local offset of the actual bottom. The offset is linearly interpolated and re-introduced into the DEM using the perimeter of a 2D hydraulic simulation of a suitably low-flow along the river. In this way, the real local width of the river is reproduced even in case that the CS_{sur} missed local enlargements or restrictions or even in presence of a braided pattern of the river. The final result is an enhanced representation of the 3D geometry of the river bed that leads to a more reliable estimates of the actual conveyance K ($m^3\ s^{-1}$) of the river. In order to provide full reproducibility, in the supplementary material the procedure is applied step-by-step to the test case of the Mella river (Northern Italy) using the freeware software QGIS and HEC-RAS. Moreover, to show clear examples of the method's applicability to riverbeds of increasing complexity, the algorithm is applied to an upland river stretch and two synthetic examples representing a braided river layout. Two executable programs to simplify some crucial tasks of the procedure are also provided along with the paper.

2. The algorithm

The proposed algorithm for the improvement of the bathymetry of a river crossing an original raster DEM (DEM_{ori}, in the following) requires the use of a GIS software and a 2D SWE solver along with a set of n_{CS} rectilinear CS_{sur} of the watercourse. A simple educated guess on a low-flow discharge is also required. In the following, the procedure is first summarized in 4 steps described in lay and visual language and then presented and applied in detail in the supplementary material.

The purpose of the first step (Fig. 1) is to identify the subset of cells of DEM_{ori} representing the river bed occupied by water during the LiDAR survey and whose elevation must be lowered. Considering the potentially arbitrarily complex outline of this area, a physically based method can work best: accordingly, a 2D simulation is performed with a suitably chosen low flow Q, such that only the riverbed as present on DEM_{ori} is flooded and the surrounding floodplain is not inundated. This step may require some simple trials. Indeed, too small discharge values would lead to the emergence of unnatural dry areas on the bed, that in case can be eliminated by post-processing, whereas too high Q values would lead to include floodplain cells that were not covered by water at the time of the LiDAR survey.

Using the results of this simulation, the shapefile of the outline of the flooded domain (SHP_{fld}) is obtained.

In the second step (Fig. 2) a set of n_{CS} cross-sections (CS_{ori}) is extracted from DEM_{ori} in correspondence with the surveyed rectilinear CS_{sur} set, limiting their transversal extent l_j (where j is the index of the CS) to the external outline of the previously identified flooded domain. Note that extending the field survey of CS_{sur} as far as the floodplain, in order to capture the levees and floodplain elevations, is a best practice: accordingly, the CS_{sur} width $L_j > l_j$. If an island is present along the cross-section, it is excluded from the computation of l_j. Then, for each cross section j, the average vertical offset Δz_j over l_j is computed as:

$$\Delta z_j = \frac{\int_{l_j} (z_{ori} - z_{sur}) d\xi}{l_j} \quad j = 1..n_{CS} \tag{1}$$

In the third step (Fig. 3), a fictitious channel is built, made up of rectangular cross sections (CS_{off}) of depth Δz_j with the same width L_j and

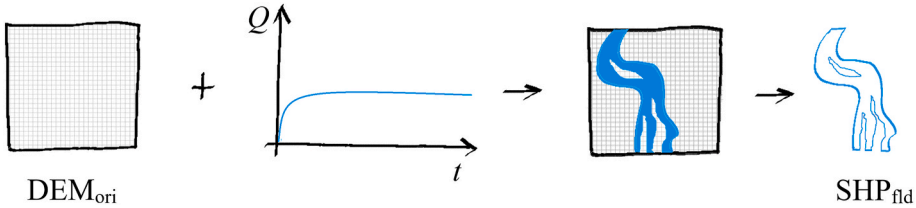

Fig. 1. Schematic of the first step of the algorithm.

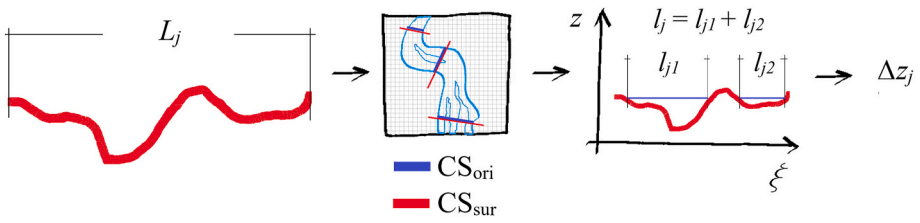

Fig. 2. Schematic of the second step of the algorithm. The blue solid segment is the outline of CS_{ori}. (For interpretation of the references to colour in this figure legend, the reader is referred to the Web version of this article. The same applies to the following figures)

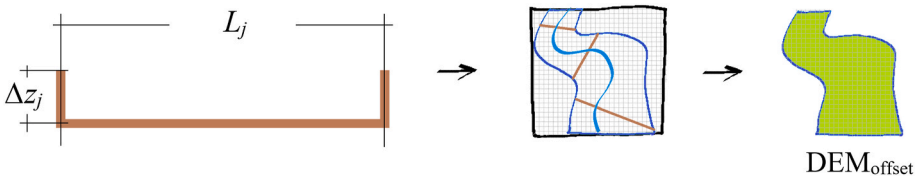

Fig. 3. Schematic of the third step of the algorithm.

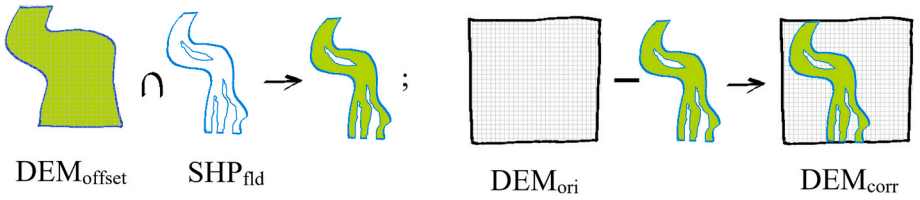

Fig. 4. Schematic of the fourth step of the algorithm.

position of the CS_{sur} set. In order to cover the actual extent of the watercourse between two consecutive CSs, these cross sections can be linearly interpolated following the centerline of the river. Then, the geometry of the fictitious offset channel is converted to a raster file, called DEM_{offset}.

Considering that the width of the channel in DEM_{offset} is locally determined by the width of CS_{sur} and is larger than the area effectively occupied by water during the LiDAR survey, in the fourth step (Fig. 4) DEM_{offset} is clipped using the polygon SHP_{fld}. Then the final corrected DEM (DEM_{corr}, in the following) is built as the difference between the elevations of DEM_{ori} and the clipped DEM_{offset}.

3. Application to the Mella river

The Mella river is a pre-alpine river in the province of Brescia, one of the most strongly urbanized areas of northern Italy. The 37-km long stretch from the village of Sarezzo as far as the village of Dello will be studied in the following. The overall river relief in the considered stretch is 230.5 m and its longitudinal profile is shown in Fig. 5. Probabilistic peak discharges at the Sarezzo station are $Q_{20} = 240\ m^3\ s^{-1}$ and $Q_{200} = 375\ m^3\ s^{-1}$ where the subscripts indicate the return period (AdbPo, 2016).

The Mella river and the surrounding floodplain is covered by a 0.8 m grid LiDAR DEM measured in 2008–2009, with planimetric and vertical accuracy of ± 0.30 m and ± 0.15 m respectively. Along the same stretch of the river, 120 CS_{sur} were surveyed in 2002, with a lateral extension that typically covers the floodplain for a width 4 times larger than the river bed; 26 CSs represent weirs and drop structures.

Considering that the LiDAR survey was accomplished in low-flow period, after a few trials, eventually a 2D simulation with a constant discharge $Q = 20\ m^3\ s^{-1}$ was performed with HEC-RAS 2D (Version 6.3.1) in order to capture the bed of the river covered by water in DEM_{ori}. A computational mesh with an average cell's area of 86 m^2 was built with local refinement up to 5 m in correspondence of levees and

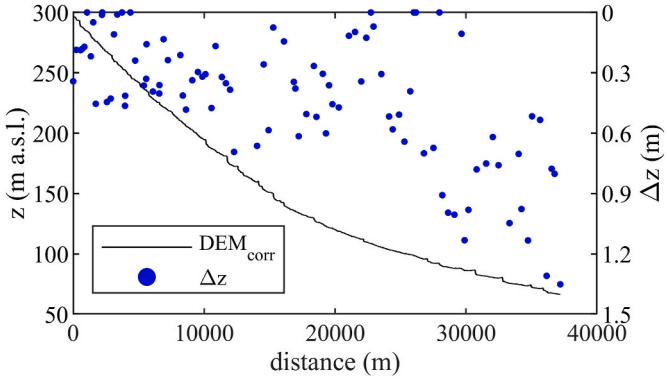

Fig. 5. Longitudinal profile of the Mella river in the investigated stretch along with computed offset Δz in correspondence of the CS_{sur} set.

other singularities. On the basis of field surveys, the Manning coefficient was set in the range $0.022 \div 0.04\ s\ m^{-1/3}$. The simulation was performed for 10 h in order to converge to the steady state solution. Using HEC-RAS Mapper, the shapefile of the flooded domain was obtained and a set of CS_{ori} in the same position of the 120 CS_{sur} with transversal width limited by the flooded domain shapefile was extracted from the DEM_{ori}. The comparison of the two sets of CSs allowed to compute the offset of the river bed for each CS (Eq. (1) and Fig. 5), with average value 0.42 m. This value and the following statistics do not account for the offset computed at the 26 CSs representing sudden drop structures where the elevation averaging over the 0.8-m grid and the possible presence of a little planimetric misalignment with CS_{sur} and CS_{ori} could introduce considerable errors in terms of offset and, consequently, in elevation. Considering the small discharge in the river presumably present at the time of the LiDAR survey, here the critical depth of the flow over the sill

was approximated to 0. Note that a small value of discharge does not imply a negligible value of the offset at other stations along the river, due to backwater effects or even local negative slopes. At the same time, the method allows different choices to be made based on the specific condition.

Although in the period 2002–2009 modifications in the thalweg profile due to sediment erosion/aggradation cannot be totally excluded, considering the limited river Mella morphodynamics it is reasonable to assume that the observed offset is mostly explained by the presence of water along the river. As one can observe, the offset increases moving downstream (Fig. 5), reflecting the decrease of the average bed slope s_b of the river and its meandering pattern in the floodplain.

The interpolation of the CS_{off} and the conversion to raster file were accomplished using HEC-RAS Mapper and the DEM_{offset} was embedded in DEM_{ori} using QGIS.

Fig. 6 shows the comparison between some cross sections extracted from DEM_{ori} and DEM_{corr} (CS_{ori} and CS_{corr}, respectively) in correspondence of CS_{sur}. The geometry of CS_{corr} is very close to the corresponding CS_{sur} one, with a very good agreement of the stage-K curves, where the conveyance K curves are computed using the software HEC-RAS as follows:

$$K(z) = \frac{1}{n} A R_h^{2/3} \tag{2}$$

where n is the Manning roughness coefficient, A and R_h are respectively the wetted area and the hydraulic radius for a fixed elevation z.

As shown by the comparison of the stage-K curves in Fig. 6, the effects of the DEM correction become more relevant as the offset increases, as typically happens where the average slope of the stretch decreases. Moreover, as one could expect, the hydraulic effect of the correction relatively decreases for growing values of the water stage.

In order to measure the quality of the reconstructed CSs, the most relevant quantity in the hydraulics of each CS, *i.e.* the conveyance, was used as a metric. Assuming the CS_{sur} as ground truth, the Root Mean Square Error (RMSE) of the conveyance has been computed for the cross sections CS_{ori} (drops excluded) as follows:

$$RMSE_{ori,j} = \sqrt{\frac{\sum_i \left(K_{ori_{i,j}} - K_{sur_{i,j}}\right)^2}{N}} \quad j = 1..n_{CS} \tag{3}$$

where, $j = 1.n_{CS}$ is the cross section and $i = 1.N$ is the number of elevation points. In a similar way $RMSE_{corr}$ has been computed for the CS_{corr} set. Fig. 7 shows the RMSE of the conveyance for the two sets of CSs.

Fig. 7 shows that at some stations the RMSE is greater for CS_{corr}. This problem is not related to the bottom correction but to some inconsistencies between the surveyed cross-section and the original DEM. An example is shown in Fig. 6d, where CS_{ori} is shallower than the surveyed one, as one could expect, but also was a bit wider. Accordingly, the wetted area of CS_{ori} for a given stage was closer to the area of CS_{sur} before the depth correction. Having corrected the bed bottom in CS_{corr}, its conveyance (see Fig. 6g) becomes larger than the real one. However, these "pathological" situations that cannot be accounted by any method, simply underline, if needed, the importance of the quality of the original data in the whole modeling process.

As a cross-validation of the proposed method, moving along the river one cross section at a time was removed and the offset was computed by linear interpolation along the river centerline between the upstream and downstream offset of the removed CS. Lastly, the RMSE was computed for the removed CS for the following comparison. To this purpose, the analysis was limited to the stretch without CS_{sur} in correspondence of sudden bed drops between 16850 and 26180 m. The adopted indicator of goodness of the cross-validation is the mean RMSE computed for the considered stretch of the river, obtaining a mean RMSE computed for CS_{ori} of 809 $m^3\ s^{-1}$, a mean RMSE for CS_{corr} of 359 $m^3\ s^{-1}$ and a mean RMSE for the cross validated offset of 545 $m^3\ s^{-1}$. Accordingly, even reducing the available information the method improves the existing geometry.

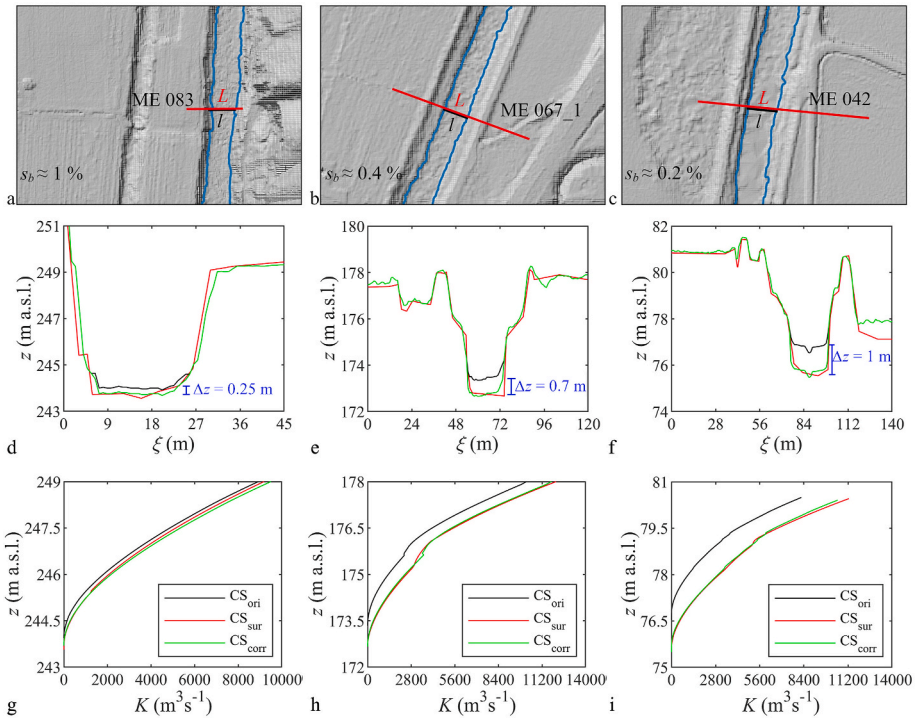

Fig. 6. Plan view of CSs ME 083 (distance = 4.7 km) (a), ME 067_1 (distance = 12.3 km) (b), and ME 042 (distance = 33.3 km) (c) from the Mella river test case with indication of the flooded area and of the part of the CS representing the riverbed. The second row shows an example of the CSs geometry extracted from DEM_{ori} and DEM_{corr} and CS_{sur}; in the third row the stage-K curves are compared to the data from CS_{sur} (d, g: CS ME 083; e, h: CS ME 067_1; f, i: CS ME 042).

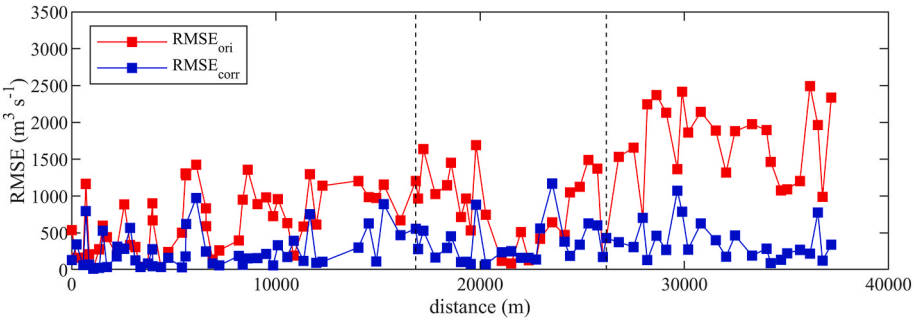

Fig. 7. RMSE of the conveyance along the Mella River for DEM_{ori} and DEM_{corr} (the vertical dashed lines enclose the stretch of the Mella River analyzed for the cross-validation).

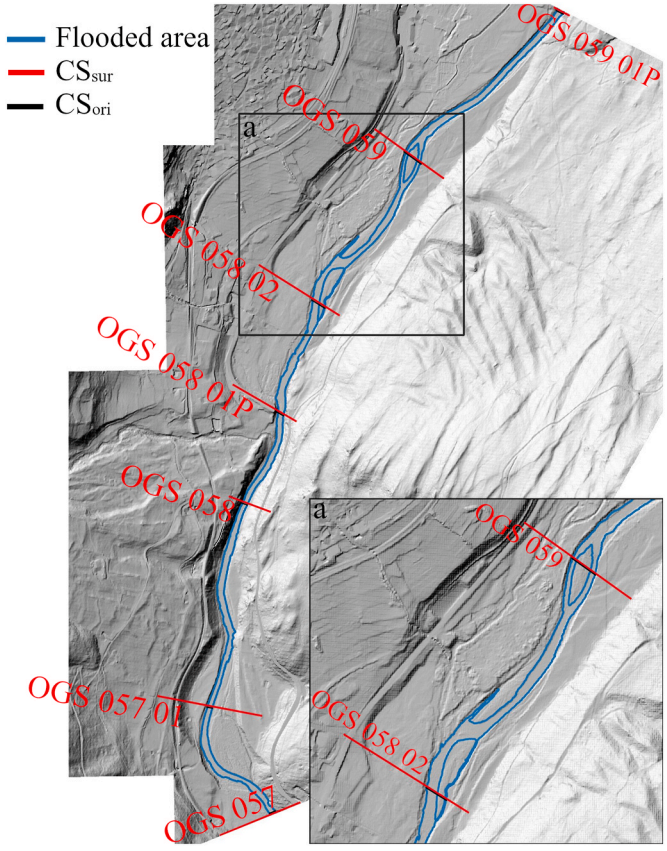

Fig. 8. Stretch of the Oglio river, highlighting the flooded area (SHP_{fld} obtained in step 1 of the procedure) and the planimetric view of CS_{sur} and CS_{ori}.

4. Discussion and conclusions

The Mella River case is characterized by a relatively simple shape of the cross sections and by the absence of islands that lead to the presence of parallel riverbeds. To evaluate the performance of the proposed methodology for a different type of river, we applied the procedure to a 2.6 km stretch (see Fig. 8) of the mountain reach of the Oglio river, in the Valle Camonica valley (Northern Italy). The investigated area is covered with a DEM (DEM_{ori}) with a spatial resolution of 0.8 m derived from a LiDAR survey carried out in 2008 and a set of 7 surveyed CS in 2002 (CS_{sur}, see also Fig. 9). The considered stretch of the river is characterized by the presence of islands in correspondence of the CSs OGS 058 02 and OGS 059, as shown in Fig. 8a.

DEM_{ori} was used as a bathymetric support to prepare a computational mesh with a grid size of 20 m, refined up to 5 m in correspondence of the river. The Manning coefficient within the bed was set in the range $0.05 \div 0.067$ s m$^{-1/3}$ on the basis of a local survey. As boundary conditions, a low-flow hydrograph with a constant discharge of 5 m^{3}s^{-1} was introduced upstream and a normal depth boundary condition with local slope of 0.02 m/m was set downstream. A 2D SWE simulation was finally accomplished using HEC-RAS 2D along the 2.6 km stretch of the Oglio river that provided the submerged part of the LiDAR only, excluding the emerging islands: from this method the CSs offsets (Δz) were computed.

Fig. 9 shows the comparison between CS_{sur} and the cross section CS_{corr} extracted from corrected DEM, along with the computed offset Δz. As one can observe, the procedure, based on a 2D simulation, corrects the DEM in the submerged part only (see OGS 059 and OGS 058 02), preserving the "true" morphology provided by the LiDAR survey and respecting the original shape of the islands.

Finally, to further emphasize the capability of the procedure to correct the bathymetry in a complex situation like that of a braided river, where any interpolation between consecutive CSs would fail, we applied it to two idealized test cases. In the first case the bathymetry shown in Fig. 10a was created, with a length of 1 km and a 0.001 m/m slope of the bottom. We used a 0.25 m grid size DEM, assuming a water depth of 0.5 m during the LiDAR survey. Fig. 10a shows the DEM of the investigated areas and the position of the 5 idealized surveyed CSs (CS_{sur}). According to the proposed procedure, a HEC-RAS 2D model of the river was built using the idealized LiDAR survey as a bathymetric support, using a computational mesh with a grid size of 2.5 m and a Manning coefficient $n = 0.03$ s m$^{-1/3}$. As boundary conditions, a low-flow hydrograph with a constant discharge of 5 m^3 s^{-1} was introduced upstream and a normal depth boundary condition with local slope of 0.001 m/m was set downstream. The comparison between CS_{sur} and the cross section CS_{corr} extracted from the corrected DEM is shown in Fig. 11.

The second paradoxical bathymetry, shown in Fig. 10b along with 6

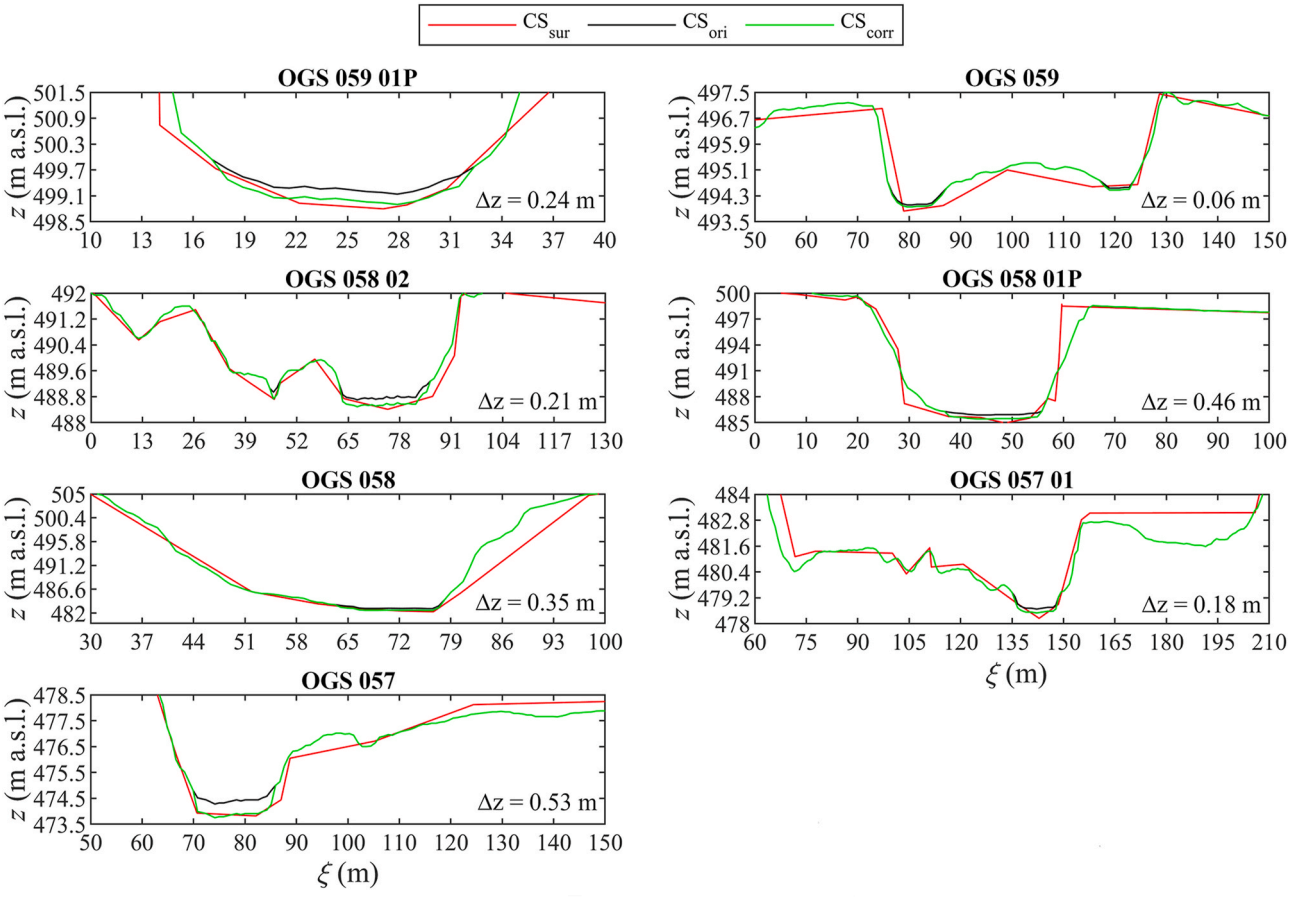

Fig. 9. Comparison between CS_{sur}, CS_{ori} and CS_{corr} for the Oglio River test case. The horizontal and vertical extent of some CSs is limited to better show the actual DEM correction.

surveyed CSs (CS_{sur}), was devised to demonstrate that the advantages of the proposed procedure grow with the complexity of the river morphology. The square 50 m × 50 m domain is characterized by a 0.05 m DEM resolution size and contains a constant water surface elevation of 1 m.

Using the same boundary conditions as before, a 2D HEC-RAS model of the stretch of the river was built using the idealized LiDAR survey as a bathymetric support and a computational mesh with a grid size of 0.5 m. Fig. 12 shows the comparison between CS_{sur} and the cross section CS_{corr} extracted from the corrected DEM. In this case, the ability of the proposed methodology to handle complex morphologies is evident. The solution provided by the SWE solver, whose streamlines are shown in Fig. 13, allows to detect automatically all the obstacles along the river and to limit the correction to the area covered by water at the time of the LiDAR survey. Note that this correction is totally unaffected by the complexity of the islands outline and by the presence of recirculation zones.

In conclusion, several methods for CS interpolation available in widely used software are excellent. For instance, HEC-RAS provides superb utilities to manage the bed bathymetry, which we used on several occasions (Pilotti et al., 2020; Milanesi and Pilotti, 2021). However, as shown in the introduction, these methods are not perfect. Considering that it is a common experience of flood modelers that the definition of accurate bathymetry is one of the most relevant and engaging steps in the whole modeling effort, we believe it is important to keep improving the available methodologies, in order to devise a method that can eventually incorporate all the constructive contributions coming from the scientific and technical discussion. The intention of this paper is to propose a possible direction for improvement.

The procedure requires only measured geometric data and an educated guess on the value of the discharge, such that in a 2D simulation only the riverbed as present on DEM_{ori} is flooded and the surrounding floodplain is not inundated. This step may require some simple trials. Moreover, it uses the simplest possible assumption on the shape of the cross-section below the water level (i.e., rectangular).

This could be a limitation if the real bathymetry significantly differs from the rectangular assumption because all the portions of CS_{ori} covered by water are translated of the same quantity Δz. On the other hand, this assumption is also the most reasonable, considering that for low stages most CSs are hydraulically wide, in the sense that their

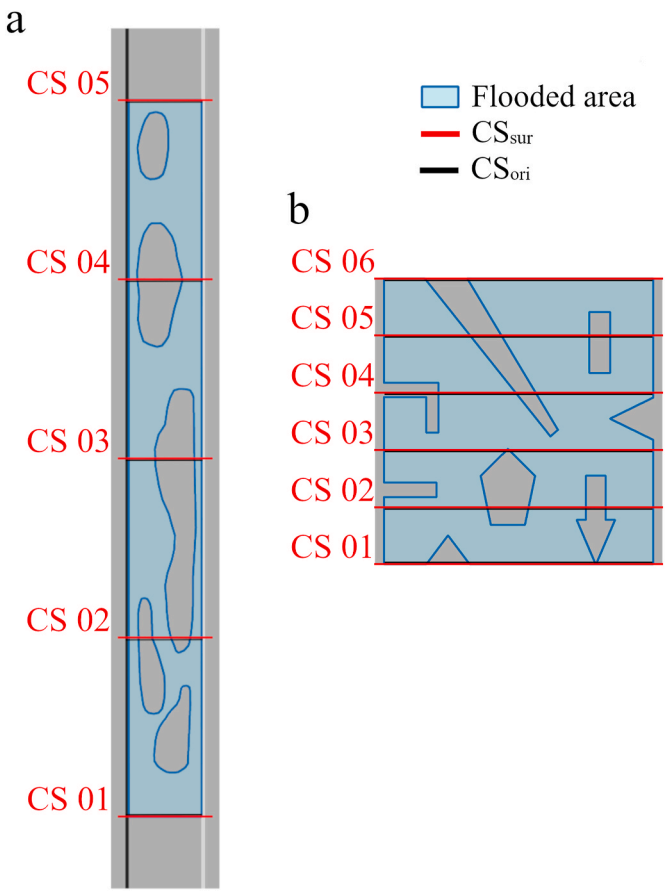

Fig. 10. Two idealized complex domains, highlighting the flooded area (SHP_{fld} obtained in step 1 of the procedure) along with the planimetric view of CS_{sur} and CS_{ori}.

hydraulic radius tends to the water depth, as in an infinitely wide rectangular CS. As a confirmation of the validity of this assumption, the mean RMSE of the conveyance for the whole Mella river stretch considering only the submerged part of each CS was computed. In this case, the mean RMSE of the conveyance computed for the CSs extracted from DEM_{corr} is 23 m^3 s^{-1}.

The methodology relies on the availability of surveyed CSs and of a DEM carefully filtered from vegetation. A reasonable density of LiDAR points inside the wetted area is also needed in order to avoid a bad representation of the water surface, that has an influence on the final shape of the reconstructed submerged part of the CS, emphasizing the importance of the good quality of the input data, without which every method is almost inevitably unsuccessful. Moreover, the importance of measuring the DEM and CSs at a short temporal distance is here underlined, in order to limit inconsistencies due to sediment transport and human modification of the riverbed.

The original DEM is modified using a 2D flood model that is also the final goal of the overall DEM improvement activities. Accordingly, this preliminary modeling effort is not to be considered as an overburden and simplified SWE models (e.g., kinematic or diffusive approximation) could well be used to this purpose. On the contrary, the 2D simulation gives a sound physical basis to the methodology and captures the river planimetric variability between two consecutive CS_{sur}, providing a reconstruction of the riverbed that preserves all the morphological information available above the water surface at the time of the survey. For instance, using the results of a 2D simulation preserves the presence of islands along the river as demonstrated by the application on a stretch of the Oglio river and on the idealized cases. The importance of using a 2D SWE simulation to provide a strong physical basis to the interpolation, was already recognized by Lai et al. (2021) who, however, in addition to the value of discharge present at the time of the survey, used the computed streamlines on a conceptualized bathymetry to recreate the intermediate CSs. Finally, the procedure presented in this paper is simpler and does not fail in presence of recirculation areas.

Provided that there is no silver bullet to solve the problem, by adding an interpolated offset to the local elevation in place of an interpolated

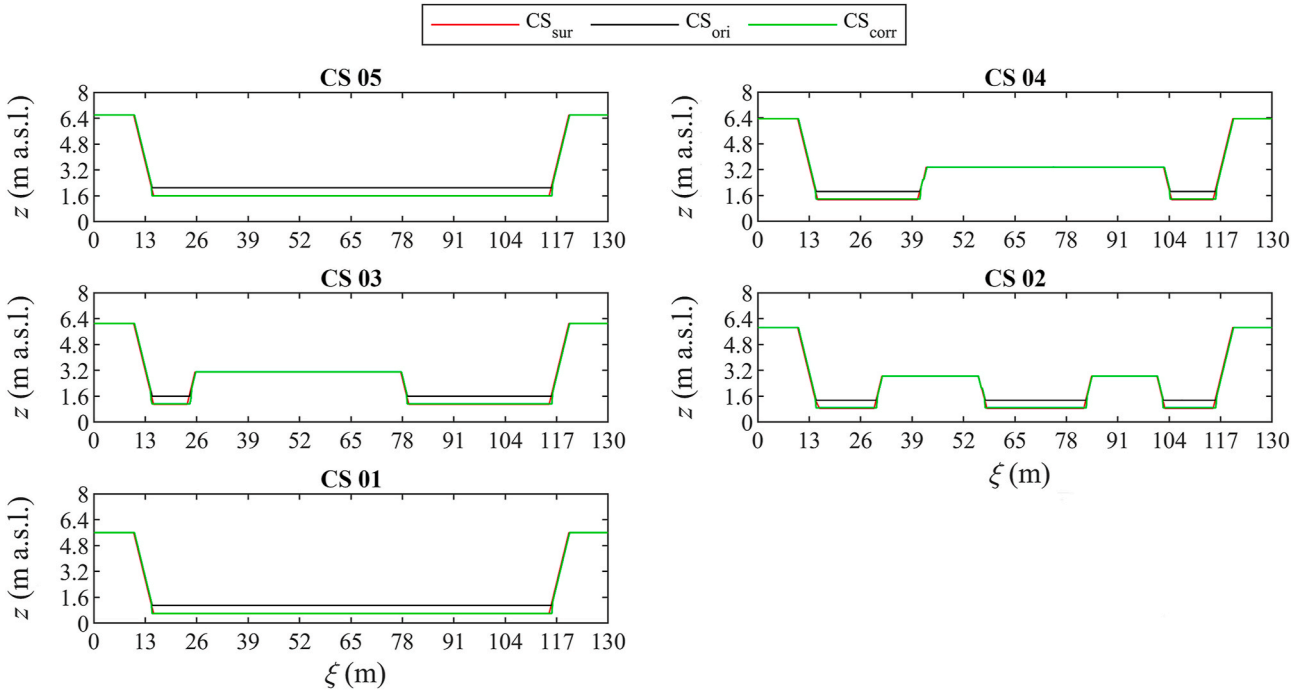

Fig. 11. Comparison between CS_{sur}, CS_{ori} and CS_{corr} for the idealized braided river test case of Fig. 10a.

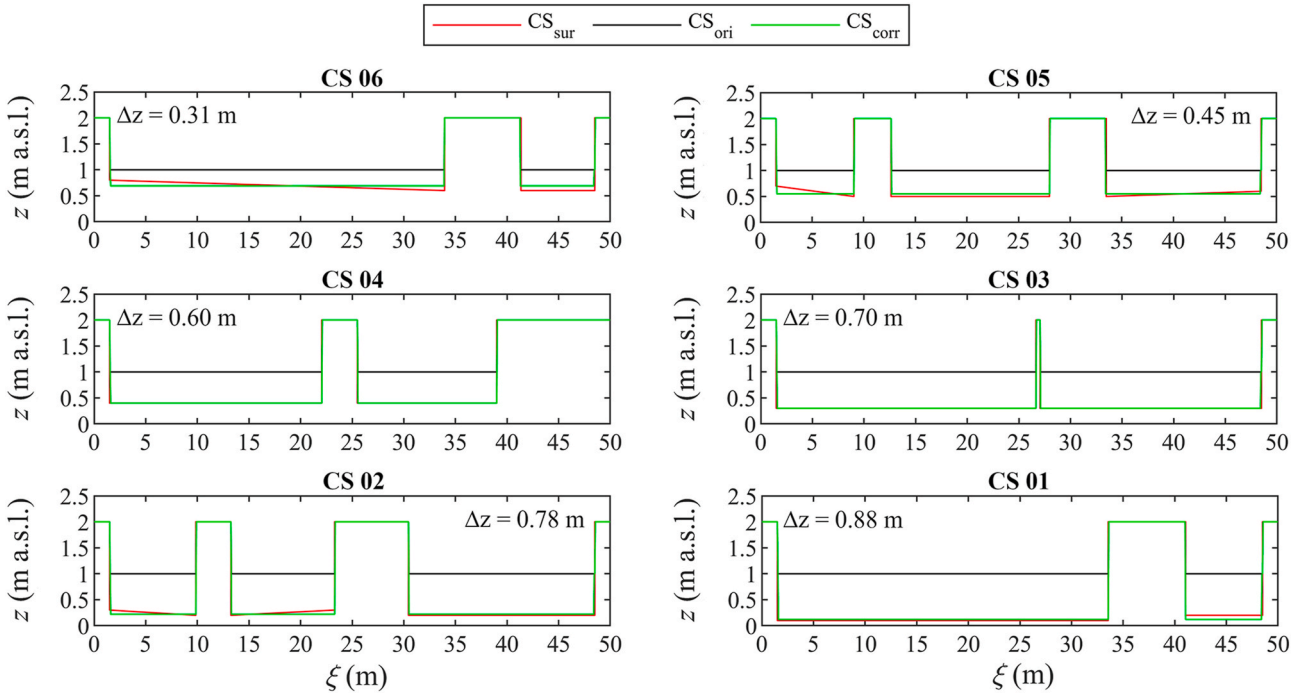

Fig. 12. Comparison between CS_{sur}, CS_{ori} and CS_{corr} for the idealized braided river test case of Fig. 10b.

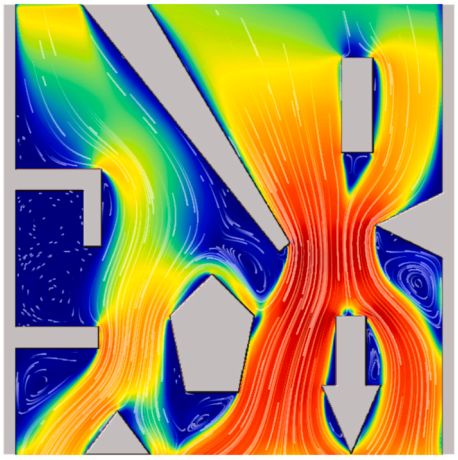

Fig. 13. Computed streamlines of the flow field for the bathymetry in the right panel of Fig. 10b. Flow from north to south.

elevation, this algorithm does not produce a uniform slope between two consecutive CS_{sur}, because it follows the measured local water surface elevation. Moreover, a 1D reconstruction of the watercourse, based on the interpolation of the CS_{sur} set only, would arbitrarily modify the CS geometry and slope between two consecutive CS_{sur}. Accordingly, we believe that the idea of "digging" the DEM inside the flooded area at the basis of the proposed methodology ensures a better consistency between the excavated area and the surrounding DEM.

Finally, the methodology can be applied using any GIS and hydraulic modeling software that allows the required operations on DEMs and CSs. To make easier its application, in the supplementary material the algorithm is implemented step-by-step using the two freeware software QGIS and HEC-RAS and two executable programs that are provided along with this paper to simplify some crucial tasks.

CRediT authorship contribution statement

Gabriele Farina: Writing – review & editing, Writing – original draft, Methodology, Investigation, Conceptualization. **Marco Pilotti:** Writing – review & editing, Writing – original draft, Supervision, Software, Methodology, Investigation, Conceptualization. **Luca Milanesi:** Writing – review & editing, Writing – original draft, Methodology, Investigation, Conceptualization. **Giulia Valerio:** Writing – review & editing, Writing – original draft, Conceptualization.

Software and data availability

- Name of software: *HECRAS_2_CSV*.exe
- Developer: M. Pilotti
- Contact: marco.pilotti@unibs.it
- Date first available: 2024
- Software required: Windows operative system
- Program language: DELPHI Object Pascal
- Source code at: https://hydraulics.unibs.it/hydraulics/tools-for-the-enhancement-of-river-bed-bathymetry-in-lidar-dem
- Documentation: Detailed documentation for application installation and testing can be found along with the supplementary material and at https://hydraulics.unibs.it/hydraulics/tools-for-the-enhancement-of-river-bed-bathymetry-in-lidar-dem
- Name of software: *Comp_CS_Offset.exe*
- Developer: M. Pilotti
- Contact: marco.pilotti@unibs.it
- Date first available: 2024
- Software required: Windows operative system
- Program language: DELPHI Object Pascal
- Source code at: https://hydraulics.unibs.it/hydraulics/tools-for-the-enhancement-of-river-bed-bathymetry-in-lidar-dem
- Documentation: Detailed documentation for application installation and testing can be found in the web page at https://hydraulics.unibs.it/hydraulics/tools-for-the-enhancement-of-river-bed-bathymetry-in-lidar-dem

Declaration of competing interest

The authors declare that they have no known competing financial interests or personal relationships that could have appeared to influence the work reported in this paper.

Acknowledgements

This research was developed within the framework of the Agreement "Metodologie per l'aggiornamento delle mappe di pericolosità idraulica", *signed with the Autorità di bacino distrettuale del fiume Po.*

Notation list

RMSE	root mean square error
Q	discharge
L	land surveyed CS total width
l	computed CS flooded width
s_b	river bed slope
K	conveyance
ξ	CS transversal coordinate
z	CS vertical coordinate
Δz	computed vertical offset
n	Manning roughness coefficient
A	wetted area
R_h	hydraulic radius
nCS	number of surveyed CSs

Appendix A. Supplementary data

Supplementary data to this article can be found online at https://doi.org/10.1016/j.envsoft.2025.106354.

Data availability

Data will be made available on request.

References

AdbPo, 2016. Piano per la valutazione e la gestione del rischio di alluvioni: Profili di piena dei corsi d'acqua del reticolo principale. Marzo 2016.

Bhuyian, M.N.M., Kalyanapu, A.J., Nardi, F., 2015. Approach to digital elevation model correction by improving channel conveyance. J. Hydrol. Eng. 20 (5). https://doi.org/10.1061/(asce)he.1943-5584.0001020.

Brunner, G.W., 2024. HEC-RAS 2D, user's manual. Exported March 2024. U.S. Army Corps of Engineers, Davis CA.

Bures, L., Roub, R., Sychova, P., Gdulova, K., Doubalova, J., 2019. Comparison of bathymetric data sources used in hydraulic modelling of floods. Journal of Flood Risk Management 12 (S1). https://doi.org/10.1111/jfr3.12495.

Castellarin, A., Di Baldassarre, G., Bates, P.D., Brath, A., 2009. Optimal cross-sectional spacing in preissmann scheme 1D hydrodynamic models. J. Hydraul. Eng. 135 (2), 96–105. https://doi.org/10.1061/(asce)0733-9429(2009)135:2(96.

Caviedes-Voullième, D., Morales-Hernández, M., López-Marijuan, I., García-Navarro, P., 2014. Reconstruction of 2D river beds by appropriate interpolation of 1D cross-sectional information for flood simulation. Environ. Model. Software 61, 206–228. https://doi.org/10.1016/j.envsoft.2014.07.016.

Conner, J.T., Tonina, D., 2014. Effect of cross-section interpolated bathymetry on 2D hydrodynamic model results in a large river. Earth Surf. Process. Landforms 39 (4), 463–475. https://doi.org/10.1002/esp.3458.

Dysarz, T., 2018. Development of RiverBox—an ArcGIS toolbox for river bathymetry reconstruction. Water 10 (9), 1266. https://doi.org/10.3390/w10091266.

Kinzel, P.J., Legleiter, C.J., Nelson, J.M., 2013. Mapping River bathymetry with a small footprint green LiDAR: applications and Challenges 1. JAWRA Journal of the American Water Resources Association 49 (1), 183–204. https://doi.org/10.1111/jawr.12008.

Knighton, D., 1998. Fluvial Forms and Processes. Edward Arnold, London.

Lai, R., Wang, M., Yang, M., Zhang, C., 2018. Method based on the Laplace equations to reconstruct the river terrain for two-dimensional hydrodynamic numerical modeling. Comput. Geosci. 111, 26–38. https://doi.org/10.1016/j.cageo.2017.10.006.

Lai, R., Wang, M., Zhang, X., Huang, L., Zhang, F., Yang, M., Wang, M., 2021. Streamline-based method for reconstruction of complex braided river bathymetry. J. Hydrol. Eng. 26 (5). https://doi.org/10.1061/(asce)he.1943-5584.0002080.

Legleiter, C.J., 2012. Remote measurement of river morphology via fusion of LiDAR topography and spectrally based bathymetry. Earth Surf. Process. Landforms 37 (5), 499–518. https://doi.org/10.1002/esp.2262.

Leopold, L.B., Maddock, T., 1953. Hydraulic Geometry of Stream Channels and Some Physiographic Implications. U.S. Government Printing Office, Washington, DC.

Mazzoleni, M., Paron, P., Reali, A., Juizo, D., Manane, J., Brandimarte, L., 2020. Testing UAV-derived topography for hydraulic modelling in a tropical environment. Nat. Hazards 103 (1), 139–163. https://doi.org/10.1007/s11069-020-03963-4.

Mersel, M.K., Smith, L.C., Andreadis, K.M., Durand, M.T., 2013. Estimation of river depth from remotely sensed hydraulic relationships. Water Resour. Res. 49 (6), 3165–3179. https://doi.org/10.1002/wrcr.20176.

Merwade, V., Cook, A., Coonrod, J., 2008. GIS techniques for creating river terrain models for hydrodynamic modeling and flood inundation mapping. Environ. Model. Software 23 (10–11), 1300–1311. https://doi.org/10.1016/j.envsoft.2008.03.005.

Milanesi, L., Pilotti, M., 2021. Coupling flood propagation modeling and building collapse in flash flood studies. J. Hydraul. Eng. 147 (12). https://doi.org/10.1061/(asce)hy.1943-7900.0001941.

Pilotti, M., 2016. Extraction of cross sections from digital elevation model for one-dimensional dam-break wave propagation in mountain valleys. Water Resour. Res. 52 (1), 52–68. https://doi.org/10.1002/2015wr017017.

Pilotti, M., Milanesi, L., Bacchi, V., Tomirotti, M., Maranzoni, A., 2020. Dam-Break wave propagation in alpine valley with HEC-RAS 2D: experimental cancano test case. J. Hydraul. Eng. 146 (6). https://doi.org/10.1061/(asce)hy.1943-7900.0001779.

Reil, A., Skoulikaris, Ch, Alexandridis, T.K., Roub, R., 2018. Evaluation of riverbed representation methods for one-dimensional flood hydraulics model. Journal of Flood Risk Management 11 (2), 169–179. https://doi.org/10.1111/jfr3.12304.

Roub, R., Hejduk, T., Novák, P., 2012. Automating the creation of channel cross section data from aerial laser scanning and hydrological surveying for modeling flood events. J. Hydrol. Hydromechanics 60 (4), 227–241. https://doi.org/10.2478/v10098-012-0020-5.

Tarpanelli, A., Camici, S., Nielsen, K., Brocca, L., Moramarco, T., Benveniste, J., 2021. Potentials and limitations of Sentinel-3 for river discharge assessment. Adv. Space Res. 68 (2), 593–606. https://doi.org/10.1016/j.asr.2019.08.005.